Journal of Thermal Analysis and Calorimetry (2020) 139:3309–3315
https://doi.org/10.1007/s10973-019-08706-7

Nanomaterial thermal treatment along a permeable cylinder

Yong Li[1] · Farshad Shakeriaski[2] · Azeez A. Barzinjy[3,4] · Rebwar Nasir Dara[5] · Ahmad Shafee[6] · Iskander Tlili[7,8]

Received: 22 May 2019 / Accepted: 15 August 2019 / Published online: 26 August 2019

Abstract

The goal of the current article is investigating the nanomaterial stream and its thermal features on a cylinder which is porous. Nanofluid viscosity and the efficient thermal conductivity are computed by KKL equation. In such method, impact of Brownian movement is incorporated. The governing PDEs will be decreased to an ODEs set with the adequate ones utilizing resemblance transformation, numerically resolved by fourth-order Runge–Kutta method. Results for flow as well as heat transfer specifications are acquired to different amounts of the nanoparticle mass fraction, *Re*, suction factor and various forms of nanofluid. In this study, such results illustrate that a nanoparticle presence in the basis fluid can alter the flow model. Based on the achievements, *Nu* is a growing function of fraction of nanoparticle, *Re* and suction factor.

Keywords Nanomaterial · Stretching permeable cylinder · Heat transfer · KKL

Introduction

In recent years, there has been being a need to improve new forms of liquids that will be more influential in heat transfer efficiency, as increasing requests of such modernistic technology as microelectronics, chemical products and power station. The general definition of nanofluid is a fluid including nano-size solid particles existing in such basis fluid with slight thermal conductivity such as oils, ethylene glycol and water [1–5]. Choi and Eastman [6] proposed the phrase of ‘nanofluid’ when they were representing a new method to augment thermal feature of HTF (heat transfer fluid). In the past years, the endeavors for improving the conduction of fluid were conducted by mixing solid particles in micrometer or millimeter sizes into typical carrier fluid; nonetheless, such method because of suspending millimeter- or micrometer-sized solid particles in fluid brings about some challenges—including channel blocking, sedimentation and abrasion—which are then resolved by reducing the size of such particles to nanometer scales, which is around 1 to 100 nm. The types of utilized nanofluids are typically metals such as Cu and Au, oxide metals such as CuO, TiO_2, Fe_3O_4 and Al_2O_3 and nonmetallic element such as carbon [7–12]. The inclusion of such nanoparticles leads the thermal conductivity of nanofluid to grow, as those nanoparticles have a greater level of thermal conductivity compared to the basis fluids [13–21].

Al_2O_3 nanofluid with 1.0% of mass concentration including a particle size of 50 nm has been utilized by Senthil et al. [22] who found that the maximum efficiency was acquired at 75% charging rate and 30° slop angle. Scientists paid attention to the most increase in thermal

✉ Iskander Tlili
iskander.tlili@tdtu.edu.vn

1 State Key Laboratory of Oil and Gas Reservoir Geology and Exploitation, Chengdu University of Technology, Chengdu 610059, China

2 Gol-Gohar Mining and Industrial Company (Gohar Ravesh Company), Sirjan, Iran

3 Computer Department, Cihan University-Erbil, Erbil, Iraq

4 Physics Department, College of Education, Salahaddin University, Erbil, Kurdistan Region, Iraq

5 Department of Petroleum Engineering, College of Engineering, Knowledge University, Erbil, Iraq

6 Public Authority of Applied Education and Training, College of Technological Studies, Applied Science Department, Shuwaikh, Kuwait

7 Department for Management of Science and Technology Development, Ton Duc Thang University, Ho Chi Minh City, Vietnam

8 Faculty of Applied Sciences, Ton Duc Thang University, Ho Chi Minh City, Vietnam

resistance, applying a various desirable mixture of disparate terms. Wei et al. [23] scrutinized the efficiency of nanomaterial within a pipe with mount of device with new shape for producing swirl flow. Ferrofluid migration with considering radiation was examined by Sheikholeslami and Shamlooei [24], and they concluded that Lorentz force makes velocity to decline. Huminic et al. [25] have conducted research about the usages of Fe_2O_3/H_2O nanomaterial in a thermosyphon heat pipe. Nanomaterials of various fractions—such as 0%, 2% and 5.3%—have been charged in the pipe. Based on their results, the most rate of performance was related to the concentration of 5.3%. Sheikholeslami et al. [26] employed nanopowder for boiling phenomena and suggested empirical correlations. The efficiency of collector employing ZrO_2/H_2O and Ag/water nanomaterial was performed by Hussain et al. [27] who illustrated that those nanofluids grew the efficiency of unit than water, no more so than at a great inlet temperature; nevertheless, the performance of that collector silver nanopowder has been greater compared to ZrO_2/water nanofluid. Other techniques were incorporated by researchers to augment performance [28–41]. The thermal efficiency as well as hydraulic efficiency of graphene nanoplatelets at different fluxes of heat flux has been computed by Arshad and Ali [42]. Based on their results, a growth in heat flux damages the nanofluid stability which is a reason for a reduction in thermal efficiency of nanofluid in a greater level of heat flux. The decrease in wall base temperature was 3.45%, and that reduction was 17.48% for thermal resistance compared to pure water. Melting of nanomaterial within a duct as a part of ventilation unit was simulated by Sheikholeslami et al. [43], and they provide second law analysis for all cases. Pressure drop and thermal feature of a coiled tube by applying alumina nanomaterial were studied by Kumar et al. [44] who found the Δp of 0.8% nanofluids to be 9%, greater compared to H_2O. The empirical *Nu* for 0.1%, 0.4% and 0.8% nanofluids has been found to be 28%, 36% and 56%, respectively, greater than basis fluid. These improvements happened because of the greater rate of k_{nf}, efficient fluid combination and storage secondary stream style in duct. It is found that the amount of thermal efficiency coefficient was higher than unity. As a result, alumina nanomaterial can be utilized as a carrier fluid in helical pipe to improve the rate of heat transfer with slight pressure fall. Improving numerical approaches helps the designers to find the optimized design for heating systems [45–66]. To augment the efficiency of cooling unit, Sheikholeslami et al. [67] suggested inserting complex turbulator and they considered exergy loss in their modeling. Mixture of R-11 with titanium was applied by Naphon et al. [68], and they conduct some experiments for various tilt angles from 0° to 90°. Based on their results, the most thermal efficiency of heat pipe has been acquired at 50% charging mass and 60° tilt angle. To gain a more fundamental insight into the mechanisms of heat transfer in nanofluids, molecular dynamics simulations are proved to be a proper technique [69, 70]. Solar unit enhanced with twisted tape has been scrutinized by Farshad and Sheikholeslami [71], and they found the best model for turbulent modeling. The entropy production through nanofluid filled

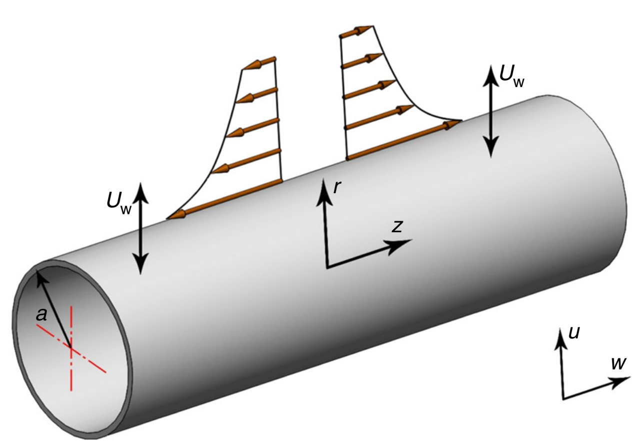

Fig. 1 Geometry of cylinder in the current study

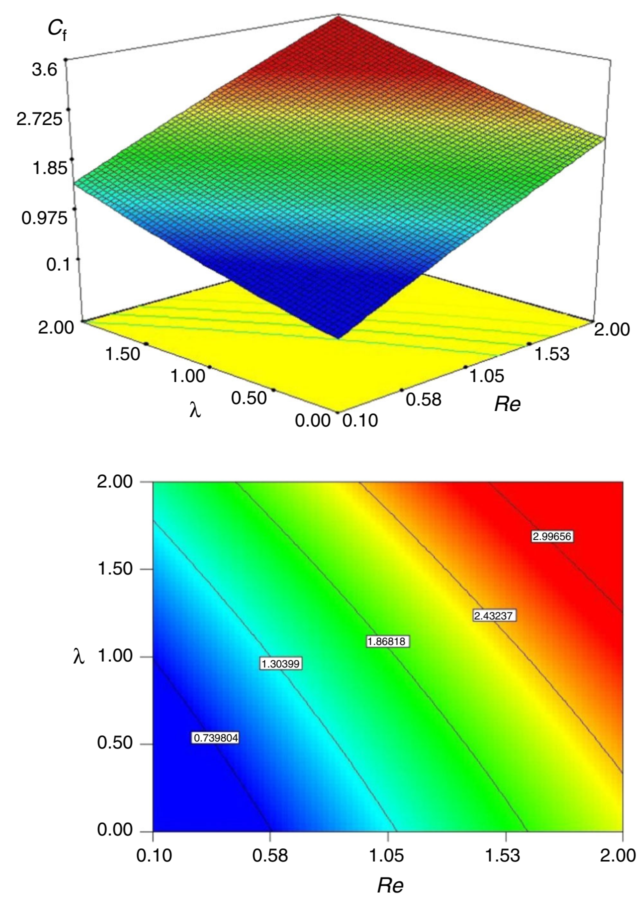

Fig. 2 Influences of λ and Re on C_f when $\phi = 0.02$

direct adsorption solar collector with Cu/water as operant fluid has been surveyed by Parvin et al. [72] in different solid mass fractions. The most efficient heat transfer factor improvement has been related to the greatest *Re* and mass fraction of 3%. This should be said that the efficiency of collector doubled.

The topic of this study is investigating the nanoparticle stream and its heat transfer because of a cylinder including an identical suction. Nanofluid viscosity and efficient thermal conductivity are computed by KKL equation. In this pattern, Brownian movement impact on the efficient thermal conductivity is taken into account. The declined ODEs are numerically resolved applying fourth-order Runge–Kutta method. The influences of factors governing on this problem are investigated and presented.

Mathematic description

Figure 1 illustrates a steady laminar nanofluid stream resulted from a stretching pipe (radius = a in axial axis). *Z*-direction as well as *r*-direction is evaluated along the direction of the pipe and in the radial one, respectively.

The viscous waste is supposed to be negligible, and tube surface is considered to have a fixed temperature T_w which is larger than T_∞. The basis fluid and the powders were in thermal balance, in which no any slip exists among them. The correlations are represented as follows under such presumptions [73]:

$$\frac{\partial P}{\partial r}+\rho_{nf}\left(u\frac{\partial u}{\partial r}+w\frac{\partial u}{\partial z}\right)=\left(-\frac{u}{r^2}+\frac{\partial^2 u}{\partial r^2}+\frac{1}{r}\frac{\partial u}{\partial r}\right)\mu_{nf}, \quad (1)$$

$$\rho_{nf}\left(u\frac{\partial w}{\partial r}+w\frac{\partial w}{\partial z}\right)=\left(\frac{\partial^2 w}{\partial r^2}+\frac{\partial w}{\partial r}\frac{1}{r}\right)\mu_{nf}, \quad (2)$$

$$\frac{\partial(ru)}{\partial r}+\frac{\partial(rw)}{\partial z}=0, \quad (3)$$

$$\left(u\frac{\partial T}{\partial r}+\frac{\partial T}{\partial z}w\right)=\left(\rho C_p\right)_{nf}^{-1}\left(\frac{1}{r}\frac{\partial T}{\partial r}+\frac{\partial^2 T}{\partial r^2}\right)k_{nf}, \quad (4)$$

$$\begin{array}{lll} r\to\infty: & T\to T_\infty, & w\to 0,\\ r=a: & T=T_w,\ w=w_w, & u=U_w \end{array} \quad (5)$$

$w_w=2zc, U_w=-a\gamma c$, and c is a positive fixed.

The carrier fluid is water, and the selected nanopowders are the same of [74], and also we utilized the KKL model for prediction of feature of nanomaterial. We supposed that mixture of copper oxide and base fluid is homogeneous.

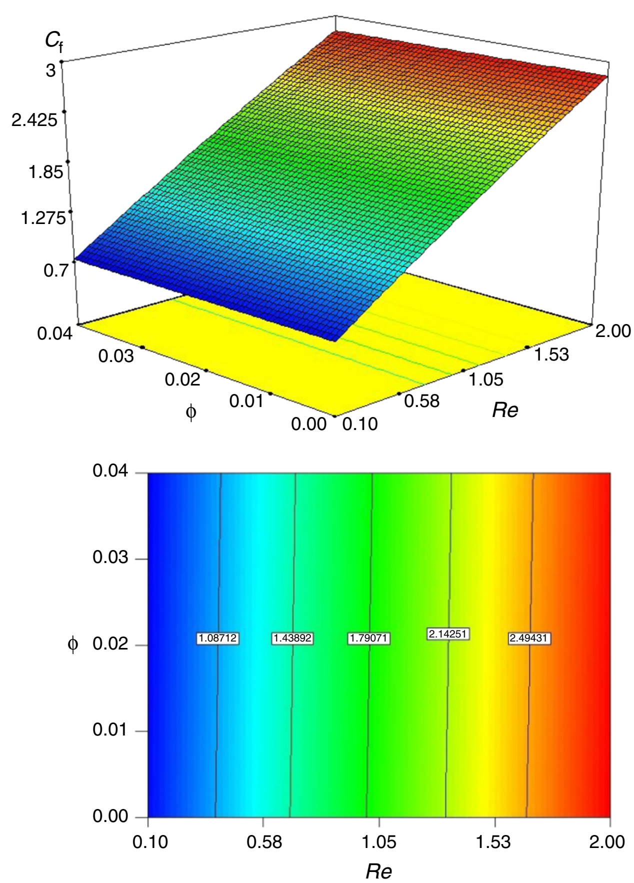

Fig. 3 Influences of ϕ and *Re* on C_f when $\lambda = 1$

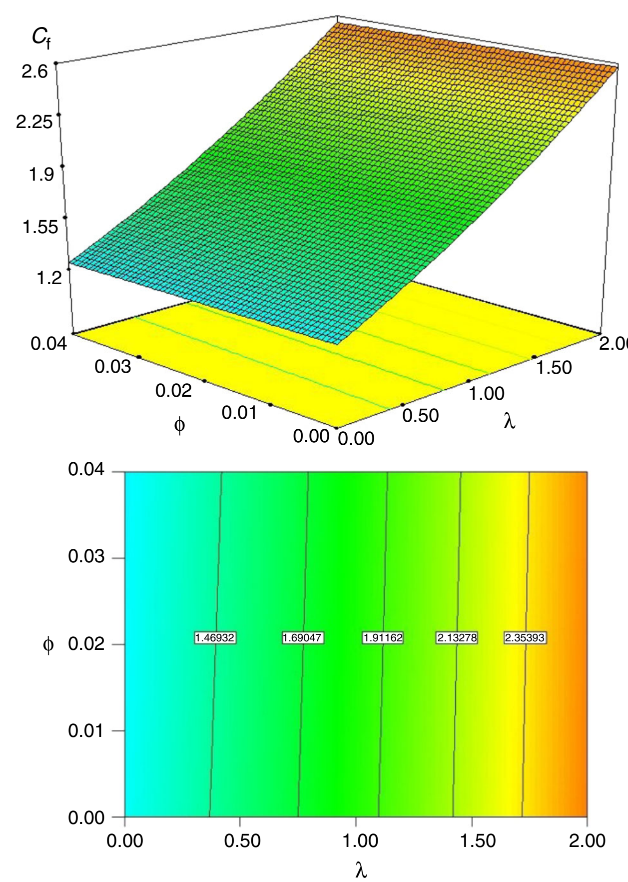

Fig. 4 Influences of λ and ϕ on C_f when Re = 1.05

The resembling transformation is considered as follows based on Wang [75]:

$$u = -ac[\eta^{-0.5} f(\eta)], \quad \eta = (r/a)^2, \\ \theta(\eta) = (T_\infty - T)/(T_\infty - T_w), \quad w = 2zcf'(\eta), \tag{6}$$

ODEs are acquired as follows by replacing Eq. (8) into Eq. (5):

$$f'' + f'''\eta = Re \cdot A_1 \cdot (1-\phi)^{2.5}\left(-ff'' + f'^2\right), \tag{7}$$

$$\eta\theta'' + (PrRef\, A_3^{-1} A_2 + 1)\theta' = 0, \tag{8}$$

$$f(1) = \gamma, \\ \theta(\infty) \to 0, \quad \theta(1) = 1, \\ f'(1) = 1, \quad f'(\infty) \to 0, \tag{9}$$

where parameters should be calculated as:

$$Pr = \mu_f (k_f \rho_f)^{-1} \left(C_p \rho\right)_f,\ A_3 = \frac{k_{nf}}{k_f} Re = ca^2/2\upsilon_f, \\ A_2 = \frac{(\rho C_p)_{nf}}{(\rho C_p)_f},\ A_1 = \frac{\rho_{nf}}{\rho_f} \tag{10}$$

Physical numbers of interest are the Nu and C_f, introduced as follows [73]:

$$Nu \equiv \frac{k_{nf}}{k_f}(-2)\theta'(1) \\ C_f \equiv \left|\left(A_1^{-1}(1-\phi)^{-2.5}\right) f''(1)\right|, \tag{11}$$

Results and discussion

On a stretching cylinder which is porous, nanofluid stream and its heat transfer are studied. The related correlations and the boundary conditions have been altered to ODEs, numerically solved by applying fourth-order Runge–Kutta method. Figures 2, 3 and 4 demonstrate the effects of ϕ, λ and Re on C_f. Also influences of scrutinized parameters on Nu are illustrated in Figs. 5, 6 and 7. Dispersion of nanoparticles becomes a significant approach in heating and cooling processes. When CuO is mixed with water, the greater Nusselt amount and lower surface friction factor can be reached. It is observed that the width of thermal boundary reduces and there is a ignorable change in the profile of velocity as the nanofluid mass fraction grows from 0 to 0.04. Temperature and velocity reduce when Re

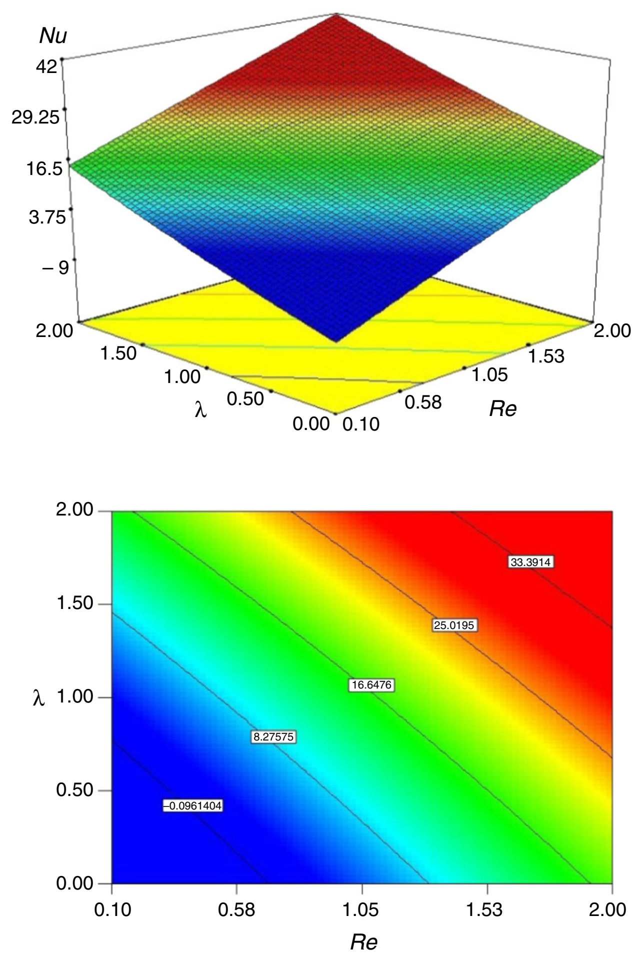

Fig. 5 Influences of λ and Re on Nu when $f = 0.02$

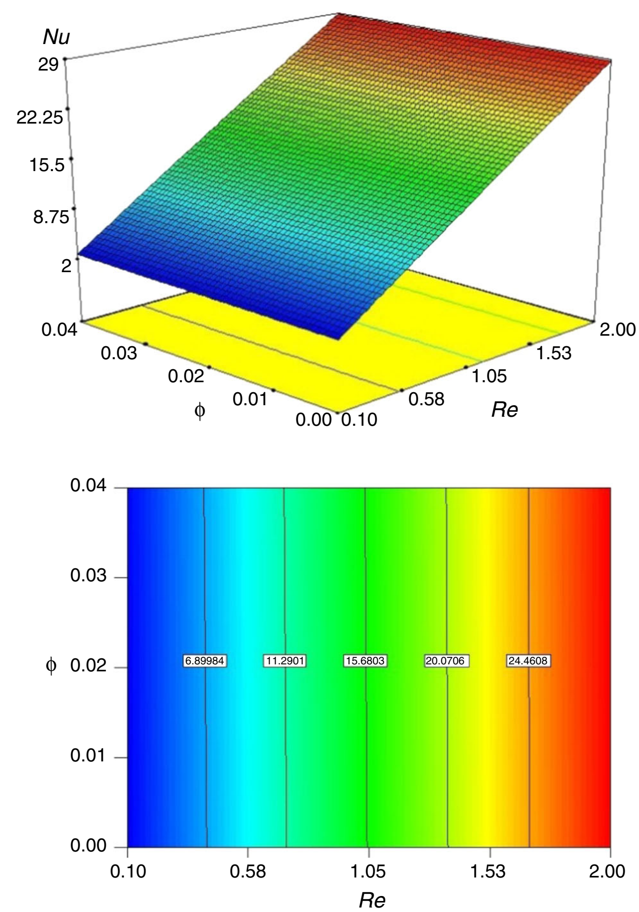

Fig. 6 Influences of ϕ and Re on Nu when $\lambda = 1$

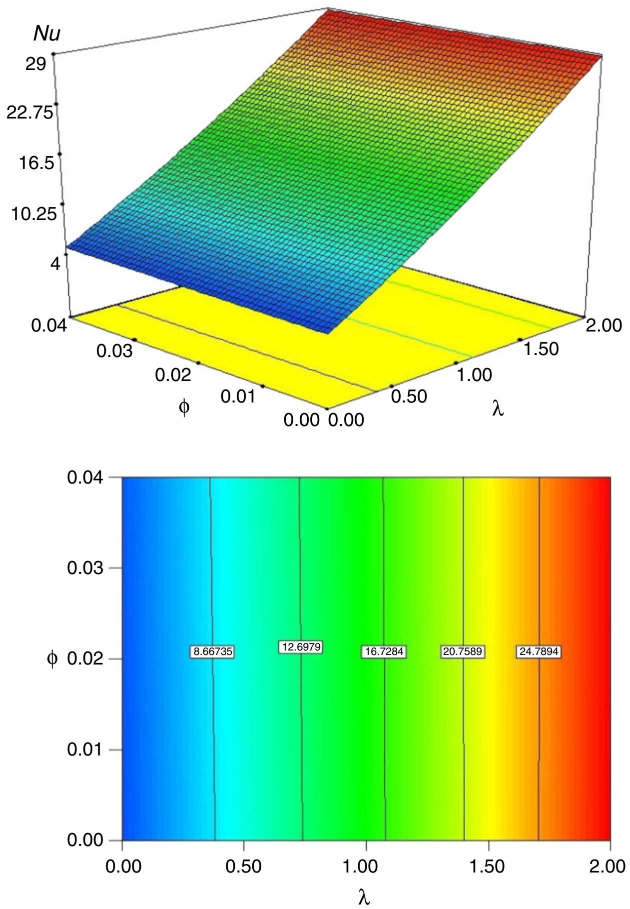

Fig. 7 Influences of λ and ϕ on Nu when Re = 1.05

rises. This resulted that surface friction factor reduces with growing mass fraction of nanofluid; nonetheless, it rises when *Re* and suction factor grow. The impacts of *Re*, nanoparticle mass fraction and suction factor on *Nu* and C_f can be summarized in two formulas:

$$C_f = 1.83 + 1.04Re + 0.65\lambda - 0.013\phi - 1.39 \times 10^{-3} Re\,\phi + 1.98 \times 10^{-3}\phi\lambda - 0.45Re^2 + 0.079\lambda^2 \quad (12)$$

$$Nu = 15.85 + 13.11Re + 12\lambda + 0.057\phi - 0.032Re\phi - 0.089\phi\lambda - 0.14Re^2 + 0.93\lambda^2 \quad (13)$$

As λ augments, velocity gradient enhances and it makes the Fanning factor to augment. C_f augments with the rise of *Re* which is attribute to higher velocity gradient. Influence of nanopowder concentration on C_f is negligible as depicted in outputs. As a consequence of augmenting λ, thinner boundary layer will be obtained and it enhances the *Nu*. *Nu* tends to decline with the decrease of *Re* and similar trend was exhibited for fraction of nanofluid.

Conclusions

This paper surveyed two-dimensional nanofluid stream because of a stretching penetrable pipe. Numerically, the equations are resolved by utilizing the fourth-order Runge–Kutta procedure. The impacts of mass fraction of nanofluid, suction factor, *Re* on the stream and its heat transfer specifications were investigated. Based on results, there is a direct communication between surface friction factor and *Re* and suction factor; nevertheless, the inverse communication is observed with mass fraction of nanofluid. Also, the width of thermal boundary layer reduces when nanofluid mass fraction, suction factor and *Re* rise. Opting higher fraction of CuO leads to greater *Nu*.

References

1. Jafaryar M, Sheikholeslami M, Li Z, Moradi R. Nanofluid turbulent flow in a pipe under the effect of twisted tape with alternate axis. J Therm Anal Calorim. 2019;135(1):305–23. https://doi.org/10.1007/s10973-018-7093-2.
2. Farshad SA, Sheikholeslami M. Simulation of exergy loss of nanomaterial through a solar heat exchanger with insertion of multi-channel twisted tape. J Therm Anal Calorim. 2019. https://doi.org/10.1007/s10973-019-08156-1.
3. Sheikholeslami M, Haq RU, Shafee A, Li Z, Elaraki YG, Tlili I. Heat transfer simulation of heat storage unit with nanoparticles and fins through a heat exchanger. Int J Heat Mass Transf. 2019;135:470–8.
4. Sheikholeslami M, Sheremet MA, Shafee A, Li Z. CVFEM approach for EHD flow of nanofluid through porous medium within a wavy chamber under the impacts of radiation and moving walls. J Therm Anal Calorim. 2019. https://doi.org/10.1007/s10973-019-08235-3.
5. Sheikholeslami M, Shafee A, Zareei A, Haq RU, Li Z. Heat transfer of magnetic nanoparticles through porous media including exergy analysis. J Mol Liq. 2019;279:719–32.
6. Choi SUS, Eastman JA, Enhancing thermal conductivity of fluids with nanoparticles, United States; 1995. https://www.osti.gov/biblio/196525-enhancing-thermal-conductivity-fluids-nanoparticles.
7. Sheikholeslami M, Mehryan SAM, Shafee A, Sheremet MA. Variable magnetic forces impact on magnetizable hybrid nanofluid heat transfer through a circular cavity. J Mol Liq. 2019;277:388–96.
8. Gao W, Wang WF. The eccentric connectivity polynomial of two classes of nanotubes. Chaos Solitons Fractals. 2016;89:290–4.
9. Sheikholeslami M, Rokni HB. Magnetic nanofluid flow and convective heat transfer in a porous cavity considering Brownian motion effects. Phys Fluids. 2018;30:1. https://doi.org/10.1063/1.5012517.
10. Sheikholeslami M, Jafaryar M, Shafee A, Li Z. Nanofluid heat transfer and entropy generation through a heat exchanger considering a new turbulator and CuO nanoparticles. J Therm Anal Calorim. 2019. https://doi.org/10.1007/s10973-018-7866-7.
11. Gao W, Zhu LL, Wang KY. Ranking based ontology scheming using eigenpair computation. J Intell Fuzzy Syst. 2016;31(4):2411–9.

12. Sheikholeslami M, Jafaryar M, Ali JA, Hamad SM, Divsalar A, Shafee A, Nguyen-Thoi T, Li Z. Simulation of turbulent flow of nanofluid due to existence of new effective turbulator involving entropy generation. J Mol Liq. 2019;291:111283.
13. Sheikholeslami M, Mahian O. Enhancement of PCM solidification using inorganic nanoparticles and an external magnetic field with application in energy storage systems. J Clean Prod. 2019;215:963–77.
14. Sheikholeslami M, Darzi M, Sadoughi MK. Heat transfer improvement and pressure drop during condensation of refrigerant-based nanofluid, an experimental procedure. Int J Heat Mass Transf. 2018;122:643–50.
15. Sheikholeslami M. Magnetic source impact on nanofluid heat transfer using CVFEM. Neural Comput Appl. 2018;30(4):1055–64.
16. Gao W, Wang WF. Analysis of k-partite ranking algorithm in area under the receiver operating characteristic curve criterion. Int J Comput Math. 2018;95(8):1527–47.
17. Sheikholeslami M, Haq RU, Shafee A, Li Z. Heat transfer behavior of nanoparticle enhanced PCM solidification through an enclosure with V shaped fins. Int J Heat Mass Transf. 2019;130:1322–42.
18. Gao W, Yan L, Shi L. Generalized Zagreb index of polyomino chains and nanotubes. Optoelectron Adv Mater Rapid Commun. 2017;11(1–2):119–24.
19. Sheikholeslami M, Gerdroodbary MB, Moradi R, Shafee A, Li Z. Application of neural network for estimation of heat transfer treatment of Al_2O_3–H_2O nanofluid through a channel. Comput Methods Appl Mech Eng. 2019;344:1–12.
20. Gao W, Guo Y, Wang KY. Ontology algorithm using singular value decomposition and applied in multidisciplinary. Clust Comput J Netw Softw Tools Appl. 2016;19(4):2201–10.
21. Sheikholeslami M. Numerical modeling of nano enhanced PCM solidification in an enclosure with metallic fin. J Mol Liq. 2018;259:424–38.
22. Senthil R, Ratchagaraja D, Silambarasan R, Manikandan R. Contemplation of thermal characteristics by filling ratio of Al_2O_3 nanofluid in wire mesh heat pipe. Alex Eng J. 2016;55(2):1063–8.
23. Wei S, Jafaryar M, Sheikholeslami M, Shafee A, Nguyen-Thoi T, Yazdani TM, Tlili I, Li Z. Simulation of nanomaterial turbulent modeling in appearance of compound swirl device concerning exergy drop. Phys A Stat Mech Appl. 2019;534:122121.
24. Sheikholeslami M, Shamlooei M. Fe_3O_4–H_2O nanofluid natural convection in presence of thermal radiation. Int J Hydrog Energy. 2017;42(9):5708–18.
25. Huminic G, Huminic A, Morjan I, Dumitrache F. Experimental study of the thermal performance of thermosyphon heat pipe using iron oxide nanoparticles. Int J Heat Mass Transf. 2011;54(1):656–61.
26. Sheikholeslami M, Rezaeianjouybari B, Darzi M, Shafee A, Li Z, Nguyen TK. Application of nano-refrigerant for boiling heat transfer enhancement employing an experimental study. Int J Heat Mass Transf. 2019;141:974–80.
27. Hussain HA, Jawad Q, Sultan KF. Experimental analysis on thermal efficiency of evacuated tube solar collector by using nanofluids. Sol Energy. 2015;4:19–28.
28. Sheikholeslami M, Jafaryar M, Shafee A, Li Z, Haq RU. Heat transfer of nanoparticles employing innovative turbulator considering entropy generation. Int J Heat Mass Transf. 2019;136:1233–40.
29. Qin Y, Liang J, Yang H, Deng Z. Gas permeability of pervious concrete and its implications on the application of pervious pavements. Measurement. 2016;78:104–10.
30. Gao W, Wang WF. The vertex version of weighted wiener number for bicyclic molecular structures. Comput Math Methods Med. 2015;418106:10. https://doi.org/10.1155/2015/418106.
31. Sheikholeslami M. Application of Darcy law for nanofluid flow in a porous cavity under the impact of Lorentz forces. J Mol Liq. 2018;266:495–503.
32. Qin Y, Hiller JE. Understanding pavement-surface energy balance and its implications on cool pavement development. Energy Build. 2014;85:389–99.
33. Sheikholeslami M, Jafaryar M, Shafee A, Li Z. Simulation of nanoparticles application for expediting melting of PCM inside a finned enclosure. Phys A. 2019;523:544–56.
34. Sheikholeslami M. Numerical approach for MHD Al_2O_3-water nanofluid transportation inside a permeable medium using innovative computer method. Comput Methods Appl Mech Eng. 2019;344:306–18.
35. Sheikholeslami M. Lattice Boltzmann method simulation of MHD non-Darcy nanofluid free convection. Phys B. 2017;516:55–71.
36. Qin Y. Urban canyon albedo and its implication on the use of reflective cool pavements. Energy Build. 2015;96:86–94.
37. Sheikholeslami M. Solidification of NEPCM under the effect of magnetic field in a porous thermal energy storage enclosure using CuO nanoparticles. J Mol Liq. 2018;263:303–15.
38. Qin Y, Zhang M, Mei G. A new simplified method for measuring the permeability characteristics of highly porous media. J Hydrol. 2018;562:725–32.
39. Sheikholeslami M. Magnetic field influence on CuO–H_2O nanofluid convective flow in a permeable cavity considering various shapes for nanoparticles. Int J Hydrog Energy. 2017;42:19611–21.
40. Sheikholeslami M. Investigation of Coulomb forces effects on ethylene glycol based nanofluid laminar flow in a porous enclosure. Appl Math Mech (English Edition). 2018;39(9):1341–52.
41. Sheikholeslami M. Finite element method for PCM solidification in existence of CuO nanoparticles. J Mol Liq. 2018;265:347–55.
42. Arshad W, Ali HM. Graphene nanoplatelets nanofluids thermal and hydrodynamic performance on integral fin heat sink. Int J Heat Mass Transf. 2017;107:995–1001.
43. Sheikholeslami M, Jafaryar M, Shafee A, Li Z. Hydrothermal and second law behavior for charging of NEPCM in a two dimensional thermal storage unit. Chin J Phys. 2019;58:244–52.
44. Kumar PCM, Kumar J, Tamilarasan R, Nathan SS, Suresh S. Heat transfer enhancement and pressure drop analysis in a helically coiled tube using Al_2O_3/water nanofluid. J Mech Sci Technol. 2014;28(5):1841–7.
45. Qin Y, Liang J, Tan K, Li F. A side by side comparison of the cooling effect of building blocks with retro-reflective and diffuse-reflective walls. Sol Energy. 2016;133:172–9.
46. Sheikholeslami M, Shehzad SA, Li Z, Shafee A. Numerical modeling for Alumina nanofluid magnetohydrodynamic convective heat transfer in a permeable medium using Darcy law. Int J Heat Mass Transf. 2018;127:614–22.
47. Gao W, Wang WF. Second atom-bond connectivity index of special chemical molecular structures. J Chem. 2014;906254:8. https://doi.org/10.1155/2014/906254.
48. Sheikholeslami M. New computational approach for exergy and entropy analysis of nanofluid under the impact of Lorentz force through a porous media. Comput Methods Appl Mech Eng. 2019;344:319–33.
49. Gao W, Siddiqui MK, Imran M, Jamil MK, Farahani MR. Forgotten topological index of chemical structure in drugs. Saudi Pharm J. 2016;24(3):258–64.
50. Qin Y, Zhang M, Hiller JE. Theoretical and experimental studies on the daily accumulative heat gain from cool roofs. Energy. 2017;129:138–47.
51. Sheikholeslami M. Influence of magnetic field on nanofluid free convection in an open porous cavity by means of Lattice Boltzmann Method. J Mol Liq. 2017;234:364–74.

52. Gao W, Liang L, Xu TW, Zhou JX. Tight toughness condition for fractional (g, f, n)-critical graphs. J Korean Math Soc. 2014;51(1):55–65.
53. Sheikholeslami M, Vajravelu K. Nanofluid flow and heat transfer in a cavity with variable magnetic field. Appl Math Comput. 2017;298:272–82.
54. Qin Y, Zhao Y, Chen X, Wang L, Li F, Bao T. Moist curing increases the solar reflectance of concrete. Constr Build Mater. 2019;215:114–8.
55. Gao W, Wang WF. Binding number and fractional (g, f, n', m)-critical deleted graph. Ars Comb. 2014;113A:49–64.
56. Sheikholeslami M, Zeeshan A. Analysis of flow and heat transfer in water based nanofluid due to magnetic field in a porous enclosure with constant heat flux using CVFEM. Comput Methods Appl Mech Eng. 2017;320:68–81.
57. Qin Y, He Y, Hiller JE, Mei G. A new water-retaining paver block for reducing runoff and cooling pavement. J Clean Prod. 2018;199:948–56.
58. Sheikholeslami M, Zareei A, Jafaryar M, Shafee A, Li Z, Smida A, Tlili I. Heat transfer simulation during charging of nanoparticle enhanced PCM within a channel. Phys A Stat Mech Appl. 2019;525:557–65.
59. Gao W, Liang L, Xu TW, Zhou JX. Degree conditions for fractional (g, f, n', m)-critical deleted graphs and fractional ID-(g, f, m)-deleted graphs. Bull Malays Math Sci Soc. 2016;39:315–30.
60. Sheikholeslami M. Numerical simulation of magnetic nanofluid natural convection in porous media. Phys Lett A. 2017;381:494–503.
61. Qin Y. A review on the development of cool pavements to mitigate urban heat island effect. Renew Sustain Energy Rev. 2015;52:445–59.
62. Gao W, Guirao JLG, Wu HL. Two tight independent set conditions for fractional (g, f, m)-deleted graphs systems. Qual Theory Dyn Syst. 2018;17(1):231–43.
63. Sheikholeslami M. Numerical simulation for solidification in a LHTESS by means of nano-enhanced PCM. J Taiwan Inst Chem Eng. 2018;86:25–41.
64. Qin Y, Luo J, Chen Z, Mei G, Yan L-E. Measuring the albedo of limited-extent targets without the aid of known-albedo masks. Sol Energy. 2018;171:971–6.
65. Sheikholeslami M. Influence of magnetic field on Al_2O_3-H_2O nanofluid forced convection heat transfer in a porous lid driven cavity with hot sphere obstacle by means of LBM. J Mol Liq. 2018;263:472–88.
66. Qin Y, Hiller JE, Meng D. Linearity between pavement thermophysical properties and surface temperatures. J Mater Civil Eng. 2019. https://doi.org/10.1061/(ASCE)MT.1943-5533.0002890.
67. Sheikholeslami M, Jafaryar M, Hedayat M, Shafee A, Li Z, Nguyen TK, Bakouri M. Heat transfer and turbulent simulation of nanomaterial due to compound turbulator including irreversibility analysis. Int J Heat Mass Transf. 2019;137:1290–300.
68. Naphon P, Assadamongkol P, Borirak T. Experimental investigation of titanium nanofluids on the heat pipe thermal efficiency. Int Commun Heat Mass Transf. 2008;35(10):1316–9.
69. Rafatijo H, Monge-Palacios M, Thompson DL. Identifying collisions of various molecularities in molecular dynamics simulations. J Phys Chem A. 2019;123(6):1131–9. https://doi.org/10.1021/acs.jpca.8b11686.
70. Rafatijo H, Thompson DL. General application of Tolman's concept of activation energy. J Chem Phys. 2017;147:224111. https://doi.org/10.1063/1.5009751.
71. Farshad SA, Sheikholeslami M. Nanofluid flow inside a solar collector utilizing twisted tape considering exergy and entropy analysis. Renew Energy. 2019;141:246–58.
72. Parvin S, Nasrin R, Alim MA. Heat transfer and entropy generation through nanofluid filled direct absorption solar collector. Int J Heat Mass Transf. 2014;71:386–95.
73. Sheikholeslami M. Effect of uniform suction on nanofluid flow and heat transfer over a cylinder. J Braz Soc Mech Sci Eng. 2015;37:1623–33.
74. Sheikholeslami M, Jafaryar M, Li Z. Nanofluid turbulent convective flow in a circular duct with helical turbulators considering CuO nanoparticles. Int J Heat Mass Transf. 2018;124:980–9.
75. Wang CY. Fluid flow due to a stretching cylinder. Phys Fluids. 1988;31:466–8.